THE ASTROPHYSICAL JOURNAL, 545:63–76, 2000 December 10

A STRUCTURE FOR QUASARS

MARTIN ELVIS
Harvard-Smithsonian Center for Astrophysics, Cambridge, MA 02138
Received 2000 February 3; accepted 2000 August 6

ABSTRACT

This paper proposes a simple, empirically derived, unifying structure for the inner regions of quasars. This structure is constructed to explain the broad absorption line regions (BALRs) and the narrow "associated" ultraviolet and X-ray "ionized" absorbers (NALs) and is also found to explain the broad emission line regions (BELRs) and several scattering features, including a substantial fraction of the broad X-ray Fe-K emission line and the biconical extended narrow emission line region (ENLR) structures seen on large kiloparsec scales in Seyfert images.

The model proposes that a funnel-shaped thin shell outflow creates all of these features. The wind arises vertically from a narrow range of radii on a disk at BELR velocities. Radiation force then accelerates the flow radially, so that it bends outward to a cone angle of $\sim 60^\circ$ and has a divergence angle of $\sim 6^\circ$, to give a covering factor of $\sim 10\%$. When the central continuum is viewed from the side, through this wind, narrow high-ionization "associated" ultraviolet absorption lines and the X-ray "ionized absorbers" are seen, as in many low-luminosity active galactic nuclei (AGNs). When viewed end-on, the full range of velocities is seen in absorption with a large total column density, giving rise to the broad absorption line systems seen in a minority of quasars, the BAL QSOs.

The wind is both warm ($\sim 10^6$ K) and highly ionized. This warm highly ionized medium (WHIM) has a density of $\sim 10^9$ cm^{-3}, putting it in pressure equilibrium with the BELR clouds; the BELR is then a cool phase embedded in the overall outflow, avoiding cloud destruction through shear. The wind has the correct ionization parameter and filling factor for this. The high- and low-ionization zones of the BELR correspond to the cylindrical and conical regions of the wind, since the former is exposed to the full continuum while the latter receives only the continuum filtered by the former.

The warm wind is significantly Thomson thick along the radial flow direction, producing the polarized optical continuum found in BALs, but is only partially ionized, creating a broad fluorescent 6.4 keV Fe-K emission line and greater than 10 keV Compton hump. The conical shell outflow can produce a biconical matter-bounded NELR.

Luminosity-dependent changes in the structure, reducing the cylindrical part of the flow or increasing the mean angle to the disk axis and decreasing the wind opening angle, may explain the UV and X-ray Baldwin effects and the greater prevalence of obscuration in low-luminosity AGNs.

Subject headings: quasars: absorption lines — quasars: general

1. INTRODUCTION

This paper proposes a simple unifying structure for the inner regions of quasars. It is almost universally acknowledged that a massive black hole lies at the core of all quasars, and it is widely believed that this black hole is surrounded by an accretion disk that emits the powerful continuum radiation characteristic of quasars. Yet the slightly larger region around the continuum source, which produces most of the prominent and much studied emission and absorption features in quasar spectra, is not well understood. It is this region that we address.

Any model of quasars and active galactic nuclei (AGNs) needs to explain self-consistently a wide range of emission and absorption-line phenomena. At a minimum the pieces of this jigsaw puzzle include (1) the ~ 5000 km s^{-1} broad emission lines present in all AGNs, (2) the $\sim 0.1c$ ($\sim 30{,}000$ km s^{-1}) broad absorption lines seen in some 10% of quasars, and (3) the highly ionized ~ 1000 km s^{-1} outflows seen in narrow absorption lines in the ultraviolet and X-ray spectra of about half of Seyfert galaxies. This is a challenging array of observations, and they lead to constraints that are hard to satisfy. Each phenomenon has been the object of many studies that have defined its properties in detail over the last two or three decades. Still missing though is a structural and dynamic context that fits these apparently disjoint elements together (Peterson 1997; Krolik 1999). The most obvious geometries are a turbulent, spherical distribution of clouds and a rotating disk with an equatorial wind. While both structures have their successes, they also have problems. One difficulty in particular stands out: how can they explain the simultaneous presence of outflowing material at 1000 and 30,000 km s^{-1} implied by the absorption lines?

Beginning from this puzzle, we propose the following, phenomenologically based, geometric and kinematic structure. An accelerating outflow with a funnel-shaped thin shell geometry is responsible for all of these features. This is the simplest geometry that can explain both the broad and narrow absorption line observations. We find having set up this structure that it also explains a wide variety of other emission-line and scattering phenomena. With minor extensions, this structure could also explain a number of luminosity-related effects.

The scope of this paper is to outline how this structural model can link these diverse phenomena empirically. In individual areas, preceding studies have often argued for the same or related conditions. Fitting all of these areas together has not been achieved before, and it is the structure proposed here that makes this possible. Many of the details and theoretical consequences are not investigated here but are explored semiquantitatively in the following sections to

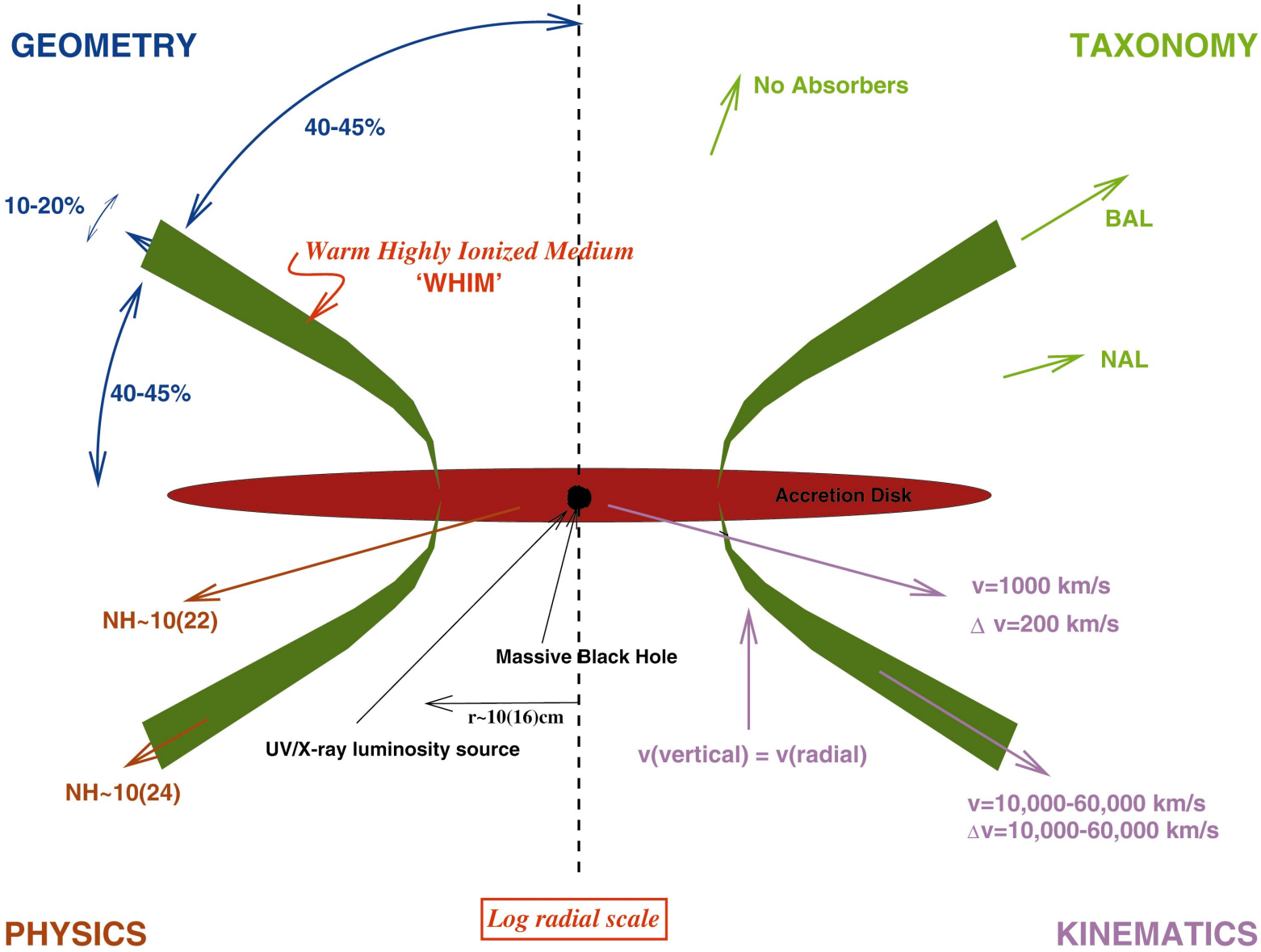

FIG. 1.—Proposed structure. The four symmetric quadrants illustrate the following (*clockwise from top left*): the opening angles of the structure, the spectroscopic appearance to a distant observer at various angles, the outflow velocities along different lines of sight, and some representative radii (appropriate for the Seyfert 1 galaxy NGC 5548) and some typical column densities.

see if obvious conflicts with observation arise. At the end of the paper some theoretical work is referred to that promises to give the model a good physical basis.

2. OVERVIEW

In outline,[1] a flow of warm gas first rises vertically from a small range of radii on an accretion disk rotating, tornado-like, with the initial Keplerian disk velocity, comparable with broad emission line (BEL) velocities. The flow then angles outward and accelerates to broad absorption line (BAL) velocities, until it makes an angle of $\sim 60^\circ$ to the quasar axis, with a divergence angle of $\sim 6^\circ$–12° (Fig. 1). Viewed along the flow a BAL is seen. Dust in low-luminosity objects prevents the BALs from being seen in Seyfert 1 galaxies. (They appear as Seyfert 2 galaxies.)

Viewed across the flow narrow absorption lines (NALs) and X-ray warm absorbers are observed. Viewed from above no absorbers are apparent. The angles are set in order to produce the correct ratios of NAL, BAL, and non-absorbed quasars. The medium is warm ($\sim 10^6$ K), has a high density ($n_e \sim 10^9$ cm^{-3}), and is highly ionized, as required by X-ray observations. We call this the warm highly ionized medium (WHIM).

These properties make the WHIM the confining medium for the clouds of the broad emission line region (BELR), for which it has the correct pressure, ionization parameter, radius, and filling factor. The BELR clouds are embedded in the WHIM and comove with the WHIM. If the wind origin radii span a factor of 2, with decreasing density at larger radii, then the two zones of the BELR have a natural origin: the high-ionization BELs originate primarily in the inner region where the clouds are exposed to the full ionizing continuum, while the low-ionization BELs originate in the outer region where they are exposed only to the continuum filtered through the WHIM. An outflowing wind with embedded cooler clouds suffers none of the shear stress problems of fast-moving clouds in a stationary atmosphere that have seemed to make pressure-confined BELR clouds implausible, and the thin shell geometry avoids the Compton depth problem previously encountered in such models. The WHIM also produces the high-ionization "coronal" optical emission lines.

Along the conical outflow direction the WHIM has significant optical depth to electron scattering ($\tau \sim 1$), as required by spectropolarimetric observations of BALs and suggested by X-ray spectra. This allows the WHIM to be the source of some, and perhaps all, of the five scattering phenomena in AGNs. Scattering off the far side of the flow explains (1) the $\sim 10\%$ polarized continuum seen in BAL troughs and the 0.5% polarization of non-BAL quasars, and (2) the strong continuum polarization in the UV. In addition, (3) the "mirror" seen in the some Seyfert 2 galaxies via polarized broad emission lines can have the same origin if, in low-luminosity AGNs, the flow is dusty. X-ray reflection features, (4) the "Compton hump" above 10 keV and (5) the fluorescent Fe-K line at 6.4 keV, will inevitably be produced from the flow. They may be sufficiently strong and of the right velocity profile to explain the revised Fe-K parameters from *ASCA*.

The model is summarized in Figure 1. The top left quadrant of Figure 1 ("geometry") shows the required angles. The top right quadrant of Figure 1 ("taxonomy") shows which lines of sight give rise to which type of absorber, while the lower right quadrant ("kinematics") shows typical velocities. The lower left quadrant ("physics") shows the relevant column densities and optical depths.

This geometry arises naturally if a disk instability creates a wind. For example, radiation pressure dominates a disk inside a critical radius. At smaller radii something (e.g., a hot corona) must suppress the wind, leaving only a narrow boundary region on the disk from which the wind can escape. Centrifugal action and radiation pressure then bend and accelerate the flow. At large radii this geometry may produce the biconical narrow emission line (NEL) structures.

High-luminosity quasars differ from the lower luminosity AGNs in several features: the lower C IV EW (Baldwin effect), the rarity of NALs, and the weakness of X-ray scattering features in high-luminosity quasars. Small changes in the outflow shape (specifically in the outflow opening angle, divergence angle, and the height of the cylindrical region) may explain these. Such shape changes could result from increased radiation or cosmic-ray pressure at high luminosities.

3. PRESENTATION OF THE QUASAR STRUCTURE

3.1. *A Conical NAL Geometry*

The intensely studied AGN NGC 5548 has had an NAL (of column density of 4×10^{21} cm^{-2}) with an outflow velocity of 1200 km s^{-1} for over 20 yr without significantly altering its high-ionization state (Shull & Sachs 1993; Mathur, Elvis, & Wilkes 1999). Yet a radial flow would have at least doubled its distance from the ionizing continuum source over this time (Fig. 2*a*; Mathur, Elvis, & Wilkes 1995), which would increase the column density in the trace C IV ion by a factor of ~ 100, contrary to observations. Continuous flow along the line of sight is ruled out, since the absorber is constrained to be thin in that direction (thickness $< 10^{15}$cm, c.f. distance from continuum equal to 2×10^{15}–2×10^{18} cm, if the UV NAL and the high-ionization [dominated by O VII, O VIII] X-ray absorption both arise in the same material;[2] Mathur et al. 1995). Instead, a steady state flow across our line of sight, with only a component of the velocity in our direction, provides a natural explanation for this constancy of ionization (Fig. 2*b*; Mathur et al. 1995, 1999).

We now note that, given the above "continuous flow" requirement, the simplest geometry for the NAL in NGC 5548 is a thin biconical shell (Fig. 2*c*) with a radial outflow velocity that will be larger, possibly much larger, than shown by the NAL. The thinness of the shell implies that the flow arises at a limited range of radii on a disk. Inevitably some lines of sight to the nucleus will not intercept the cones and so will not show absorption features. It is then simple for all AGNs to have biconical outflows. If so, then the opening angle of the conical shell is given by the ratio of NALs to absorption free AGNs (1:1) (Reynolds 1997;

[1] For brevity all references are deferred to the following detailed discussion.

[2] Statistically the UV absorption features and the X-ray warm absorbers are closely related (Crenshaw et al. 1999) and can even be used to predict one another's presence (Mathur, Wilkes, & Elvis 1998). The first *Chandra* absorption-line results (Kaastra et al. 2000; Kaspi et al. 2000) show that the high-ionization X-ray absorption lines also have outflow velocities matched to those of the UV absorbers. There remain difficulties in fitting the observed UV and X-ray line strengths with a one-component model in some cases.

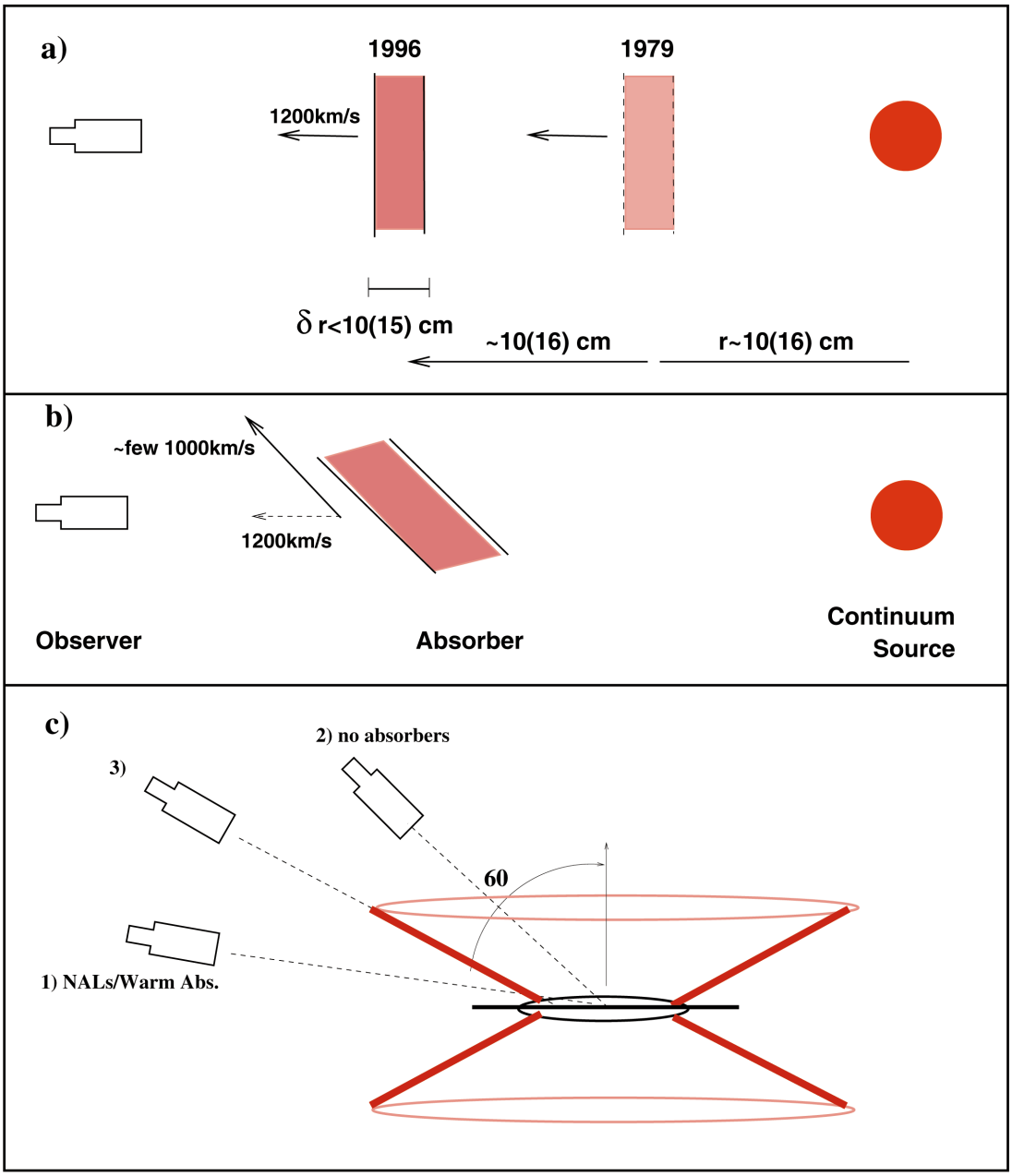

FIG. 2.—Geometry of the NAL/X-ray warm absorber. (*a*) Apparent outflow rate would double the continuum-absorber separation in 20 yr, incompatible with observations. (*b*) A steady state flow crossing our line of sight reconciles the observations. (*c*) The simplest nuclear structure compatible with (*b*) is a bicone.

Crenshaw et al. 1999). This ratio implies that the flow makes an angle of 60° to the disk axis, dividing the absorbed and unabsorbed solid angles equally (Fig. 2*c*).

3.2. *Broad and Narrow Absorption Lines: Two Views of the Same Outflow*

A conical outflow has three distinct viewing directions (§ 3.1): above the cone, across the cone, and down the length of the cone. This third view will produce higher velocity absorption in a small fraction of quasars. The flow, if accelerated by radiation pressure, must have a divergence angle, since the illumination is not parallel. For an angle of 60° to the pole, the flow will have a height comparable to its radius. The angle subtended to the accelerating continuum will be given by the thickness of the flow, which is ~0.1 radii, i.e., 6°, which implies a covering factor of ~0.1. There is a population of quasars that shows these characteristics, the BAL quasars.

All radio-quiet quasars seem to contain high-velocity outflows ($v \sim 0.1c$–$0.2c$, 10–20 times larger than NALs) as shown by studies of BALs in quasars (Weymann et al. 1991; Hamann, Korista, & Morris 1993). Any model of quasar structure must then include BAL outflows. BALs are observed directly in 10%–20% of radio-quiet AGNs and so cover a similar fraction of the solid angle around the continuum source (Weymann et al. 1991; Hamann et al. 1993). The geometry of BAL flows is not known but may well have conical shell geometries (Murray et al. 1995; Ogle 1998).

We propose that NALs and BALs are two views of the same flows. In NALs we look across the flow direction,

while in BALs we look down the length of the flow. BALs had been thought to have inadequate column densities ($\sim 10^{20}$–10^{21} cm^{-2}), similar to NALs, and relatively low ionization (Turnshek 1988). Now, however, X-ray results on BAL quasars (Mathur, Elvis, & Singh 1996; Gallagher et al. 1999; Mathur et al. 2000) strongly suggest absorbing column densities greater than or approximately a few times 10^{23} cm^{-2}, 2–3 orders of magnitude larger than expected from optical data alone. The relatively weak optical absorption then requires the BALs to have high-ionization parameters, comparable with those of NALs (Hamman 1998). The detection of Ne VIII, O VI, and Si XII in some BALs (Telfer et al. 1998) supports high–BAL ionization parameters.

Variability studies give some support for the existence of large structures in quasars on this size scale: microlensing events in the double quasar Q0957+561 contain a low-amplitude signal with delay times of 52–224 days (Schild 1996), implying luminous, possibly reflective structure with a 10% covering factor on a size scale appropriate for being the BAL outflow (see § 5); a continuum lag of 100 days is seen in NGC 3516 (Maoz, Edelson, & Nandra 2000), also implying a reflecting structure on this scale.

A covering factor of 10% for BALs implies a divergence angle of 6° (Fig. 1, *top left quadrant*, "geometry"); 20% implies a wider angle of 12°.2. Continuity implies a decreasing density in the wind with radius that will maintain a constant ionization parameter, apart from the attenuation of the ionizing radiation by absorption and scattering.

A simple bicone, though, is not compatible with the data. The velocity of the NALs, v(NAL) $\sim$ 1000 km s^{-1}, is only $\sim$1/20 that of a BAL, implying that the typical angle through the flow at which associated absorbers are found is 87°, inconsistent with the angles derived above. The simplest geometry that removes this problem is to have the flow begin as a locally vertical flow, which is appealing on the grounds of symmetry. Most NALs then arise in a quasi-cylindrical region and would be viewed almost directly across the flow (Fig. 3). The cylindrical flow is viewed in NALs between 90° and 57° (Fig. 3) for a mean angle of 80°, so the vertical outflow velocity in this region is typically some 6 times greater than the observed NAL blueshift, i.e., comparable to the BELR velocities (FWHM). A cylindrical flow will inevitably curve outward at some point as vertically displaced gas elements will have excess kinetic energy for their increased radial distance from the central mass (de Kool 1997). The whole flow then has a funnel shape.

This shape has a natural physical interpretation. Radiation or cosmic-ray pressure can cause the flow to bend radially outward and accelerate it to the large BAL velocities (de Kool 1997). In this picture the onset velocities of BALs relative to the emission-line peaks occur at the point where the flow turns outward to become part of the BAL line of sight. This will happen when the radial velocity becomes comparable with the vertical velocity (Fig. 3). The range of vertical velocities will be similar to the BAL "detachment velocities," $\sim$0–5000 km s^{-1} (Turnshek 1988; Weymann et al. 1991). N. Murray (2000, private communication) suggests that low-ionization BALs, which have narrower widths than high-ionization BALs, might arise from a shielded low-ionization region just outside the high column density X-ray "warm absorber"–producing part of the outflow, extending for about a factor of 2 in radius. This arrangement of matter proves to be valuable in understanding BELR structure, too (see § 4.1).

With the geometry of Figure 3, the thickness of the vertical region, δr, derived for NGC 5548 (§ 3.1) is 0.1r, the

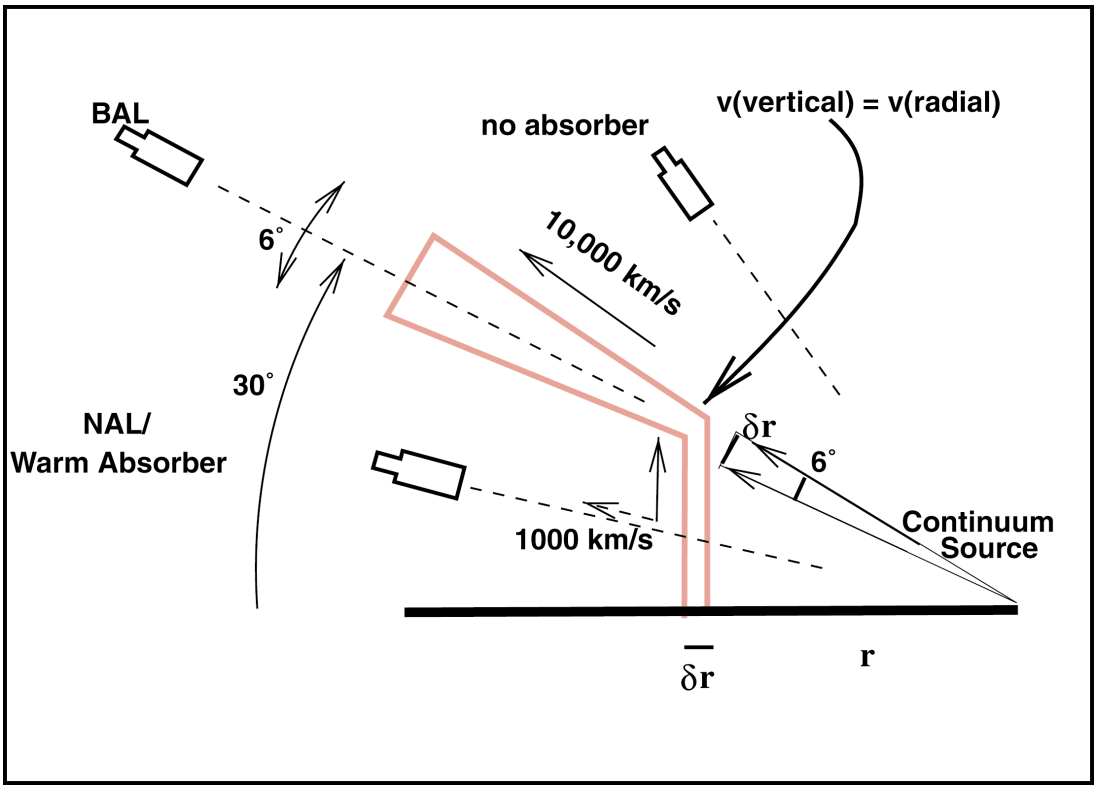

FIG. 3.—"Funnel" is the simplest geometry that allows NALs and BALs to arise in the same outflow

distance from the central continuum source. The thickness δr then subtends an angle of 6° to the continuum source, which is the divergence angle required to produce the observed fraction of BALs. The diverging continuum incident on the base of the conical outflow would then produce the observed BAL fraction, by means of radiation pressure acceleration.

4. IMPLICATIONS OF THE STRUCTURE

Given the structure just presented, other parts of the AGN puzzle fit quite naturally. Several of the solutions given below have been proposed individually before, and references are given, but they have not before all been fitted together in a single scheme, as here. The structure presented here allows the solution.

Figure 4 shows a three-dimensional rendering of the structure. The multicolored ellipse represents the accretion disk. The top panel shows the side view, viewing the continuum source through the cylindrical part of the outflow (*shown in red*), where absorption produces the NAL; the middle panel shows the view directly down the conical flow, where the accelerating flow produces a BAL spectrum; and the lower panel shows the view over the top of the flow, where there is a clear line of sight to the continuum source. Embedded in the flow are small condensations (*white dots*), which are the BEL clouds. We discuss these next.

4.1. *WHIM and BELR: Two Phases of the Same Medium*

The BAL and BEL regions are closely related. Lee & Turnshek (1995) see a correlation of their line widths. In NGC 5548 the size of the high-ionization BELR (in C IV) is 10 lt-day (Peterson 1997), $\sim 10^{16}$ cm, consistent with the distance of the WHIM from the ionizing continuum (§ 3.1; Mathur et al. 1995).

Conditions in the WHIM and BELR are also suggestively related: a strong case can be made that the WHIM is sufficiently warm and dense that it can pressure-confine the BELR clouds, as proposed here. Pressure-confined BELR models have a long history (Matthews 1974) but are not currently favored (Peterson 1997). Nevertheless, the case for high-ionization material in the vicinity of the BELR has been well argued by Shields, Ferland, & Peterson (1995), Hamann et al. (1995a), and Hamann, Zuo, & Tytler (1995b), who detected broad Ne VIII emission lines. That the NAL medium confines the BELR clouds has been suggested before (Turner et al. 1993; Kaastra, Roos, & Mewe 1995; Marshall et al. 1997). Additional evidence for high pressure, combined with the geometry proposed here, now makes the case stronger.

The evidence for the WHIM having a high pressure comes from X-ray absorption and emission features. X-ray absorption edges in some AGNs fail to respond immediately and linearly to changes in the ionizing continuum as expected in equilibrium photoionization models (Fabian et al. 1994; McHardy et al. 1995). Both nonequilibrium models and warm absorbers at $\sim 10^6$ K (where collisional ionization competes with photoionization) can reproduce these changes, and both require quite high densities, $10^6 < n_e < 10^8$ (Nicastro et al. 1999). Higher densities are needed in AGNs where no delays are seen (e.g., NGC 5548; Nicastro et al. 2000).

Strong high-ionization O VII emission lines are seen in soft X-rays in the Seyfert 1 galaxies NGC 5548 and NGC 3783 (George, Turner, & Netzer 1995; Nicastro et al. 2000;

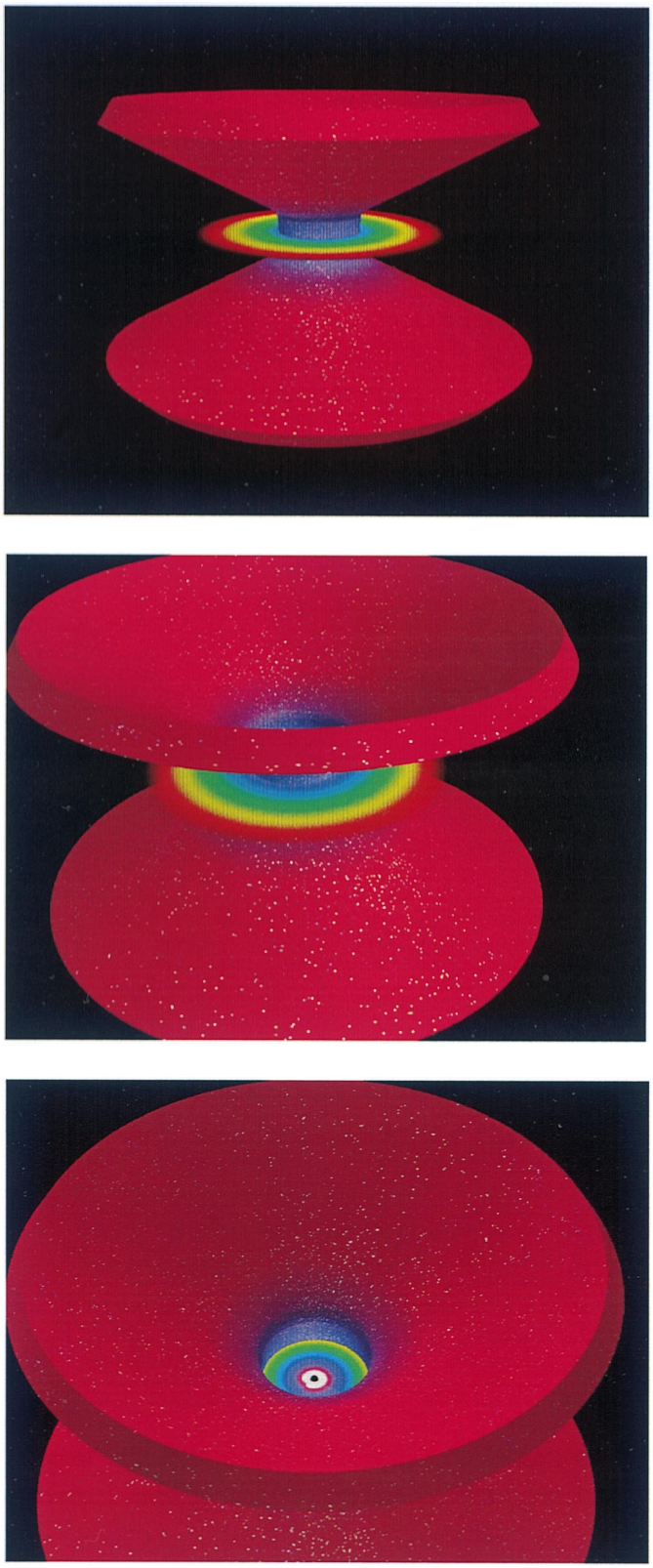

FIG. 4.—Three-dimensional views of the proposed structure. *Top:* From the side, through the NAL-producing outflow. *Middle:* Down the length of the accelerating, BAL-producing outflow toward the continuum source (note the visibility of a large area of the far side of the flow). *Bottom:* Over the top with an unobscured view of the continuum source. The multicolored disk represents the accretion disk. The small white dots represent BELR clouds embedded in the flow. (The sharp edges are an artifact of the three-dimensional rendering program.)

Kaspi et al. 2000; Kaastra et al. 2000). However, a spherical geometry would produce EUV and X-ray emission lines that were much too strong. Kaastra et al. (1995) find a filling factor for the WHIM of ~0.5%, in reasonable agreement with the 1% of a conical shell with a 6° divergence angle. To explain these lines requires a thermal ionization component at $T \sim 10^6$ K and $n_e \sim 10^9$ cm^{-3} (George, Turner, & Netzer 1995; Nicastro et al. 1999). This thermal gas has the correct ionization state and column density to produce the X-ray absorbers and the UV NALs (Kaastra et al. 1995).[3] The pressure in the WHIM of the ionized absorbers in the NGC 5548 is $P_{\rm WHIM} = 10^{15}$ cm^{-3} K, which is comparable to the pressure in the BELR (Osterbrock 1989; Ferland et al. 1992), $P_{\rm BELR,CIV} = 10^{15}$ cm^{-3} K. The factor of ~100 higher density in the BELR requires that the ionization parameters of the WHIM, $U_{\rm WHIM}$, be a factor of ~100 higher than that of the BELR, $U_{\rm BELR}$. This is close to the observed factor of 50 ($U_{\rm BELR,CIV} = 0.04$, Peterson 1993; $U_{\rm WHIM} = 2$, Mathur et al. 1995). This may well be generally true, since NALs (Crenshaw et al. 1999) have quite uniform U as do BELRs (Osterbrock 1989). Kaastra et al. (1995) find (independent of their *Extreme Ultraviolet Explorer* [*EUVE*] data) that for the observed NGC 5548 continuum a two-phase medium forms at the distance of the BELR, with $T = 5 \times 10^4$ K and $T =$ a few times 10^5 K, a slightly narrower range than above, but in good qualitative agreement, given the poorly known continuum from 100 to 912 Å.

[3] The EUV Ne VII/Ne VIII blend, Si VII emission lines reported in NGC 5548 by Kaastra et al. (1995) have been disputed by Marshall et al. (1997). However, the conditions they derive are sufficiently close to those required from the X-ray O VII and variability data that their other conclusions apply. We predict then that the lines they report will be found with observations of slightly greater sensitivity.

If the outflow spans a factor of 2 in radius, then the two BELR zones deduced from observation (Collin-Souffrin et al. 1988; Goad et al. 1999) are created naturally (N. Murray 2000, private communication). These zones are the "high"-ionization zone (e.g., C IV) and the "low"-ionization zone (e.g., Mg II) (Fig. 5), which has large optical depth and is mostly heated and ionized by hard X-rays (Collin-Souffrin et al. 1988). The WHIM filters the ionizing continuum, preventing soft X-ray flux (Ferland, Korista, & Peterson 1990) from reaching the outer radii. This is appealing since the low-ionization lines have somewhat narrower widths (FWHM) than high-ionization lines, which would arise from the $\sqrt{2}$ lower Keplerian disk velocities at double the radius and is consistent with the line width versus inverse square root of the lag time relation found for several Seyfert galaxies (Peterson & Wandel 1999; B. M. Peterson & A. Wandel 2000, in preparation). A zone of about the correct width was noted by Nicastro (2000) in his model, which relates BEL width to Keplerian disk velocity and uses the disk instability model of Witt, Czerny, & Życki (1997) (see § 6.4).

How can a factor of ~2 in radius be reconciled with the thin shell required by the X-ray observations? The thin shell applies to the high-ionization "warm absorber" zone. A lower density spanning a wider range of radii is allowed so long as the total column density through the low-ionization region is small enough not to have significant optical depth in soft X-rays, notably in oxygen, i.e., $N_{\rm H} \leq 10^{20.5}$ cm^{-2}. Since the warm absorbers have $N_{\rm H} \sim 10^{22.5}$ cm^{-2}, a strong radial density gradient in the outflow is required. In the model of Witt et al. (1997) a gradient will be present but may not be sufficiently steep (B. Czerny 2000, private communication). Evidence for cold absorption associated with warm absorbers has been seen in several

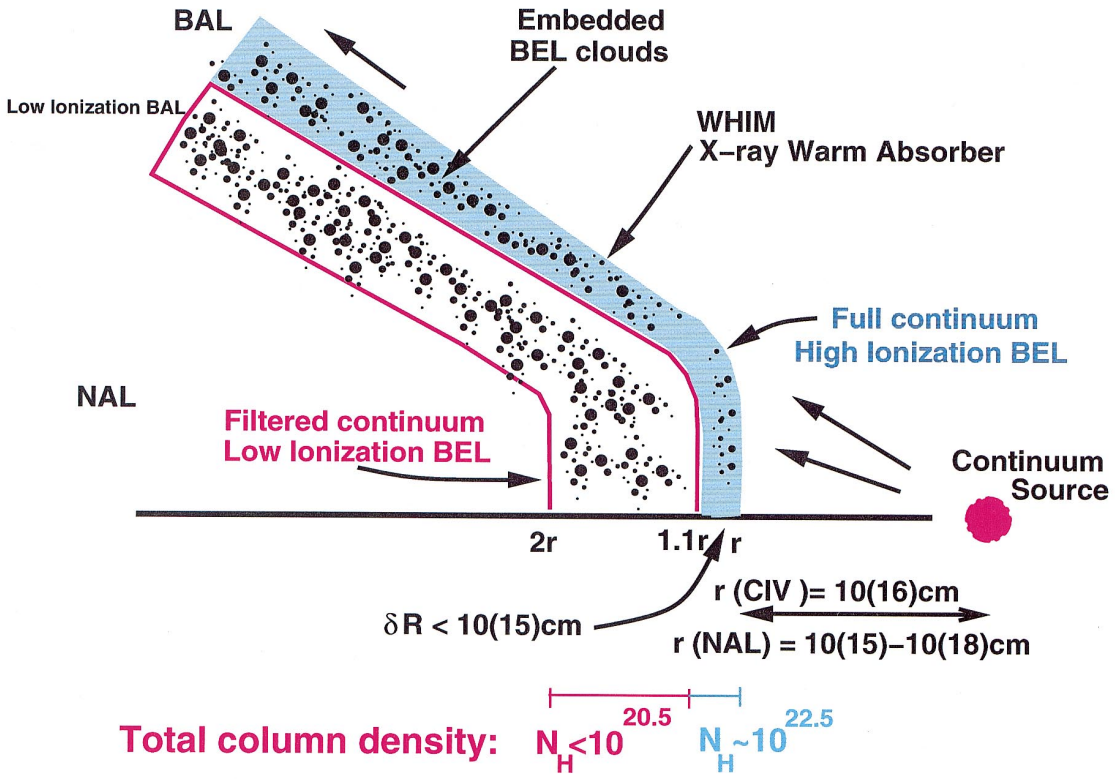

FIG. 5.—BELR as a cool phase in the WHIM outflow. Distance scales are shown for NGC 5548. The high-ionization BELR is coincident with the X-ray–absorbing WHIM, while the low-ionization BELR lies at larger radii where it is shielded, by the WHIM, from the full ionizing continuum.

X-ray spectra (Komossa 1999) and has been modeled with dust absorption, though low-N_H cold gas may also be allowed. If this is confirmed, then the steep density gradient requirement may be lessened.

Some low-ionization line emission could arise along the conical flow, several light-months away from the continuum source (for NGC 5548), which also will be shielded from the full continuum by the WHIM. Mg II in NGC 3516 has a reverberation time comparable with these sizes (Goad & Koraktar 1998). In this case, though, the WHIM is being accelerated and so the lines should appear broader. A low-contrast "very broad line region" (VBLR) is present as shown by variability (Ferland et al. 1990) and polarimetry in some AGNs (Goodrich & Miller 1994; Young et al. 1999) with about double the width of the normal (variable, unpolarized) BELR. These lines may arise in the conical flow region.

Models in which the BELR clouds are confined in pressure equilibrium in a two-phase medium (Krolik, McKee, & Tarter 1981) have fallen out of favor because of lifetime problems (Matthews 1986) and high Compton depth. In the thin shell steady state outflow picture presented here, the geometry gives a medium that has a low Compton depth except along the flow. Moreover, the individual clouds do not need long lifetimes, since they leave the BEL-emitting, vertical part of the flow on an outflow timescale, comparable to the dynamic timescale. Moreover, they are not pulled apart by strong drag forces, since they comove with the confining medium. Only a small energy input, $\sim 10^{-4}$ relative to the bulk kinetic energy of the outflow, is needed to heat the NAL gas to 10^6 K.

Radiation-driven flows commonly suffer instabilities and shocks (e.g., Williams 2000), which may well heat the WHIM (e.g., Feldmeier et al. 1997) and may also produce the fine structure in the absorption-line velocity profiles seen in NALs (Mathur et al. 1999; Crenshaw & Kraemer 1999) and BALs (Turnshek 1988). In BALs the constancy of this velocity structure (Weymann 1997) suggests standing shocks, although in NALs fine structure variability has been seen, arguing for some transverse motions (Crenshaw et al. 1999). Shock heating along the flow may also prevent the rapid adiabatic cooling of the WHIM.

If we provisionally accept the identification of the BELR as condensations in the larger WHIM outflow, is this consistent with the known properties of the BELs? Emission lines give weaker constraints than absorption lines because the information they carry has been integrated over a volume distribution of material, rather than a line, convolving together ranges of density and ionization state to produce the emission line. The prediction of BEL profiles is thus subject to the uncertainties of many parameter models. Nevertheless, a funnel-shaped distribution for the BELR seems to be consistent with the BEL profiles and widths. The distribution of BEL widths can be reproduced well by axisymmetric, but nonspherical, geometries (Rudge & Raine 1998), while the BEL profiles arise naturally in a wind (Cassidy & Raine 1993; Murray & Chiang 1995). The model predicts orientation effects in BEL profiles. Edge-on AGNs, which will show NALs, will be dominated by the disk Keplerian velocities, while pole-on AGNs, which will have no absorption features, will be dominated by the outflow velocities, both vertical and radial. Velocity-resolved reverberation mapping of the "edge-on" (because of the presence of NALs; Fig. 1, *top right quadrant*) AGN NGC 5548 (Korista et al. 1995) shows that radial motion does not dominate for the C IV line. The cylindrical structure proposed here for the high-ionization BEL will be rotating with the disk, so rotation will dominate in an NAL AGN, although a vertical velocity component will also be present. There is a tendency for high-ionization lines to be blueshifted relative to low-ionization lines (Peterson 1997; Wilkes 1984), which has no obvious interpretation in this model.

The observation that the NALs absorb the BELs (Mathur et al. 1995, 1999) presents a difficulty, since it suggests that the NAL is exterior to the BEL, rather than being commingled. Several authors have noted, though, that this problem is avoided if the BEL clouds primarily emit back toward the continuum and so are seen originating on the far side of the flow (Hamann et al. 1993; Shields 1994; Shields et al. 1995) and are seen through the near side.

5. A SINGLE COMPTON THICK SCATTERER

AGNs give ample evidence for scattering and fluorescing media: (1) BAL quasars have 5%–10% polarized flux filling in the BAL troughs (Cohen et al. 1995; Goodrich & Miller 1995; Ogle 1998), requiring an ionized medium with significant electron scattering optical depth ($\tau > 1$, $N_H > 1.5 \times 10^{24}$); (2) some type 2 Seyfert galaxies have highly polarized broad lines (Antonucci & Miller 1985; Miller & Goodrich 1990) due to electron scattering ($\tau > 0.1$) off a warm ($T \sim 3 \times 10^5$ K) medium (Miller, Goodrich, & Mathews 1991); (3) X-ray spectra of Seyfert 1 galaxies often show an excess "hump" of emission above 10 keV ascribed to Compton scattering ($\tau \gtrsim 1$) (Piro, Yamauchi, & Matsuoka 1990; Pounds et al. 1990; Lightman & White 1988); (4) a broad fluorescent Fe-K line is reported in many Seyfert 1 X-ray spectra peaking around 6.4 keV (i.e., no more ionized than Fe XVII), but extending down in a long tail to $\sim$4–5 keV (Tanaka et al. 1995; Nandra et al. 1997b) with implied Doppler velocities of up to $\sim 0.3c$; and (5) rapidly rising UV continuum polarization toward short wavelengths is seen in several quasars (Impey et al. 1995; Koratkar et al. 1995).

It seems unlikely that such an abundance of scattering phenomena should all be independent, although a priori they could be and are usually modeled as such. The X-ray features are normally, and plausibly, thought to arise in the inner regions of an accretion disk, producing general relativistically distorted radiation (Bromley, Miller, & Pariev 1998); the Seyfert 2 scatterer is believed to be an extended, 1–50 parsec scale cloud (Miller et al. 1991; Krolik & Kriss 1995); and the BAL scatterer is assumed to be part of the BAL outflow (Goodrich & Miller 1995). The UV continuum scatterer has been successfully modeled as a mildly relativistic outflowing wind from an accretion disk (Beloborodov & Poutanen 1999), a situation strongly reminiscent of the model proposed here. The WHIM outflow has many of the characteristics of all of these scatterers: high temperature and ionization, a significant Compton depth, substantial covering factor, and large velocities. The outflow must then contribute to these features. Can it explain them entirely?

5.1. *BAL Scatterer*

In a BAL quasar, where we observe down the flow, the conical shell outflow will produce an electron-scattered continuum from the far side of the outflow (Figs. 4*c* and 6),

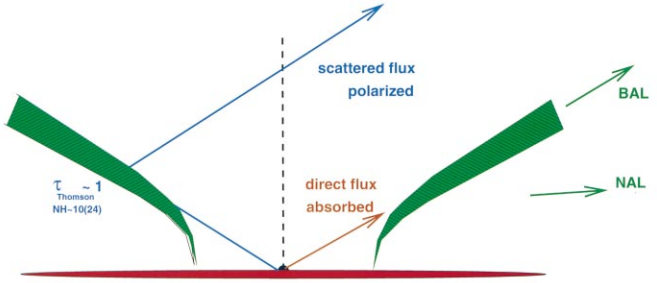

FIG. 6.—Geometry of Thomson scattering off the flow (see also Ogle 1998).

which reaches a maximum 10% polarization for a cone angle of 60° from the disk axis (Ogle 1998), the same angle we find from other considerations (see § 2). This component will appear at all energies, including X-rays, where it will reduce the apparent column density in existing X-ray spectra (Goodrich 1997b). Viewed from any non–face-on angle above the flow, this conical geometry will produce a slight net polarization that can account (Ogle 1998) for the weak (0.5% mean) optical polarization of non-BAL radio-quiet quasars (Berriman et al. 1990). Spectropolarimetry already suggests that the BAL scatterer is comparable in size to the BELR and may be cospatial (Goodrich & Miller 1995; Ogle 1997, 1998; Schmidt & Hines 1999).

5.2. *Seyfert 2 Mirror*

The "mirror" in Seyfert 2 galaxies with polarized BELs has comparable temperature, column density, and outflow velocity to the NALs (Beloborodov & Poutanen 1999; R. Antonucci 1999, private communication). If, like BALs, the "polarized BEL" Seyfert 2 galaxies are viewed end-on through the flow, then, as in BALs, the polarized emission will be scattered off the far side of the flow.

Dust may be more abundant in low-luminosity Seyfert galaxies than in quasars (Edelson, Malkan, & Rieke 1987), suggesting that Seyfert BALs are not detectable because reddening removes the UV spectrum where BALs are found, making BALs rare in Seyfert galaxies but relatively common in (radio-quiet) quasars (Turnshek 1988). (At least some of the long-sought "quasar 2 objects" [Almaini et al. 1995; Halpern & Moran 1998] are then the BAL quasars.) About 20% of Seyfert 2 galaxies have polarized BELs (Kay 1994); however, type 2 Seyfert galaxies are $\sim$4 times as common as type 1 galaxies (Huchra & Burg 1992; Rush, Malkan, & Spinoglio 1993; Comastri et al. 1995), so there are $\sim$80% as many "polarized BEL" Seyfert 2 galaxies as all Seyfert 1 galaxies, implying a covering factor close to 50% (see § 6.2). The absence of large velocity shifts in the polarized BELs of Seyfert 2 galaxies is not surprising since the opposite side of the outflow is almost perpendicular to the line of sight. Large transverse outflow velocities will produce second-order Doppler shifts. This could explain the 400 km s^{-1} redshift of polarized Hβ in NGC 1068 (Miller et al. 1991) if the transverse velocity is 15,000 km s^{-1}. Spatially resolved Seyfert 2 mirrors (Capetti, Macchetto, & Lattanzi 1997; Capetti et al. 1996) on an $\gtrsim$10 parsec scale are probably too large to be a part of this structure and have good alternative explanations (e.g., the 70 pc scale, warped molecular disk in NGC 1068; Schinnerer et al. 2000).

5.3. *X-Ray Scatterer*

The outflow matches quite well the properties of the Fe-K reflector: the WHIM has the proper ionization state (with Fe XVII dominating; Nicastro et al. 1999), and BAL widths imply that the conical outflow has a velocity spread of up to 0.2*c*, which is almost as large as the reported broad Fe-K X-ray line widths. Most BALs, though, have rather narrower widths. However, the 10%–20% covering factor of the BALs is 2–5 times lower than those of disk models and so would produce proportionately weaker Fe-K lines and Compton humps (although a covering factor closer to 50% may be more appropriate for the low-luminosity AGNs [§ 5.2], which is where broad Fe-K lines have been reported). A total of 20%–40% of the 300 eV EW Fe-K line, i.e., $\sim$100 eV, could then arise from the outflow structure.

Outflow models for the broad Fe-K lines have been considered previously: Fabian et al. (1995) noted that the strong observed red asymmetry of the broad Fe-K lines could be produced from the far side of the flow. This is tricky to arrange with the flow because it is optically thin to the fluorescence line. Resonant scattering in the highly nonspherical geometry may be able to induce an asymmetry. However, the Lubinski, Zdziarski, & Madejski (2000) results cited above seem to remove this problem in the majority of AGNs. Fabian et al. (1995) rejected outflow models both because of their ad hoc nature and because of an apparent conflict with the smaller NAL velocities seen in the same objects. Our model removes both objections (§ 3.2): the outflow is already required to explain other, quite different absorption-line phenomena, and our geometry reconciles the low absorption-line velocity across the flow, with the large emission-line velocity width integrated along the flow.

Disk models for the X-ray broad Fe-K line and Compton hump have difficulties in producing strong enough Fe-K emission lines. Several theoretical explanations have been proposed (stronger fluorescence from ionized plasma, Matt, Fabian, & Ross 1991; Życki & Czerny 1994; enhanced abundances,[4] Turnshek et al. 1996; but see Hamann et al. 1993; Lee et al. 1999; anisotropic emission, George & Fabian 1991), but all have problems.

Several sources studied in detail do not show the expected fast response of the reflection spectrum to changes in the continuum (Georgantopoulos et al. 1999; Chiang et al. 2000). IC 4329A was studied simultaneously with *ASCA* and *RXTE*, thus covering the Fe-K line and Compton hump with good signal-to-noise ratio, making this a particularly well-determined spectrum (Done, Madejski, & Życki 2000). In this observation the Fe-K line is clearly broad, but with a width of $\sim$23,000 km s^{-1}, it is distinctly narrower than a relativistic disk fit. The line also does not vary when the continuum changes by a factor of 2. In a disk-torus scenario this behavior is puzzling. If at least a substantial fraction of the broad Fe-K line arises from the Compton-thick BAL-producing outflow, which has a size of light-weeks, then the lack of response of the Fe-K line to continuum changes in these cases can be understood.

In order to explain the whole Fe-K and Compton hump, it would be necessary for the measurements to be systematically overestimating the Fe-K line strength and width. A reanalysis of the whole *ASCA* data set for AGNs (Lubinski

[4] In fact, enhancements of greater than 4 times solar are excluded by the X-ray measurements.

et al. 2000) using the "Tartarus" data base suggests that this is indeed the case. The original *ASCA* analysis, notably the comprehensive study by Nandra et al. (1997a), used a 1994 calibration that has since been improved. Lubinski et al. (2000), repeating the Nandra et al. (1997a, 1997b) analysis exactly, but with the 1996 calibration data, found that the typical Fe-K equivalent width was reduced to $\sim$100–150 eV and that the broad red wing disappeared for all but a few AGNs. MCG $-$6-30-15, the original "broad-line" Seyfert galaxy (Tanaka et al. 1995), retains a weak broad wing in this new analysis. The remaining Fe-K line is symmetric and has a Gaussian width of $\sim$0.1 keV ($\sim$5000 km s^{-1}). With these revised parameters the outflow proposed in this paper is capable of providing the whole of the observed emission line. Any further reduction in the line strength or width would in fact cause difficulties for the model.

6. DISCUSSION

6.1. *Building BAL Column Densities*

The flow geometry of Figure 1 naturally creates a larger column density along the flow than across it. Integrating the column density with mass conservation gives a factor increase of $1/\theta$ radians, where θ is the flow divergence angle. (The $1/r^2$ decrease in density renders the contributions to column density from the outer parts of the flow negligible.) For $\theta = 6^\circ$ this gives a factor of $\sim$10, i.e., 4×10^{23} atoms cm^{-2} for NGC 5548. This is somewhat less than a Thomson depth, 1.5×10^{24} atoms cm^{-2}, implying $\tau_{es} = 0.25$ and a scattering of 23% of the incident flux. This is somewhat low to create the observed scattering effects, and more detailed calculation is needed to test whether a larger column density is required.

A higher column density outflow could be created by adding mass to the WHIM. The BEL clouds offer a way of doing this. Once they enter the radial part of the flow, the BEL clouds become shielded by a larger WHIM column density, thus making the continuum they see weaker in soft X-rays. Nicastro (1995) has looked at the effect of steepening the ionizing optical–to–X-ray slope (α_{ox}) on the two-phase medium and finds that the instability disappears below some critical α_{ox}. If this applies in the conical part of the flow, then the BEL clouds will disperse, increasing the total column density. In order to increase the column density by a factor of 5–10, the mass in the BEL clouds has to be 5–10 times greater than in the WHIM. As yet there is no theory for the amount of matter that goes into each phase of a multiphase medium such as the quasar outflow or the galaxy interstellar medium, so that a factor of this size is acceptable. BEL clouds need a minimum column density of 10^{22} cm^{-2} (Krolik 1999), but there is no upper limit, and large values are sometimes invoked (Ferland et al. 1992). This allows large values of M(BEL clouds)/M(WHIM), depending on the size and number of the clouds. Using the same simplifying assumptions as Peterson (1997) and a cylinder of thickness 1/10 of its radius for the vertical part of the flow gives r(BEL cloud)/r(cylinder) $= 66 N_{\rm cloud}^{-1/3}$. So for $N_{\rm cloud} = 10^6$, r(BEL cloud)/r(cylinder) $= 0.04$ and r(BEL cloud) $= 4 \times 10^{14}$ cm, roughly 10 Schwarzschild radii (r_S) for a 10^8 $M_\odot$ black hole, as deduced to be present in NGC 5548 from reverberation mapping (Ho 1998). For 10^9 clouds these dimensions become r(BEL cloud)/r(cylinder) $= 0.004$, r(BEL cloud) $= 4 \times 10^{14}$ cm $\sim 1 r_S$. Smooth BEL profiles favor $N_c > 10^7$ (Arav et al. 1998). These then are plausible numbers.

Alternatively, there might be a reservoir of more highly ionized gas in the outflow. This is hinted at in the reports of an Fe-K absorption edge in some Seyfert galaxies (Costantini et al. 2000; Vignali et al. 2000). In this gas all elements up to iron are fully ionized. Such a medium would add to the Thomson depth and Fe-K fluorescence line strength without affecting the line absorption in soft X-rays or the UV.

6.2. *Luminosity Dependences: The Baldwin Effect*

High-luminosity quasars differ from the lower luminosity Seyfert galaxies in several ways: (1) high-luminosity quasars have weaker emission-line equivalent widths, especially high-ionization emission lines (Osmer & Shields 1999; Espey & Andreadis 1999), than low-luminosity quasars (the "Baldwin Effect"; Baldwin 1977); (2) in X-rays the weakness of Fe-K lines and Compton humps in quasars is consistent with the Baldwin effect (Iwasawa & Taniguchi 1993; Nandra et al. 1997a); and (3) NALs (in either UV or X-rays) are rare in quasars but common in the lower luminosity Seyfert galaxies (Mathur et al. 1999; Nicastro et al. 1999).

We suggest that these three luminosity-dependent effects are directly related to changes in the funnel geometry (Fig. 7). The angles derived so far (Fig. 7*b*) depend primarily on the statistics of NALs among Seyfert 1 galaxies, which are AGNs of relatively modest luminosity. If the quasi-vertical flow region is smaller at high luminosities (perhaps because radiative acceleration is stronger for high-luminosity objects), then a smaller solid angle will be exposed to the unattenuated continuum source, weakening the BELR, particularly the high-ionization lines. There will also then be a smaller solid angle from which the continuum can be viewed through the WHIM, so NALs will be rarer. If the cone opening angle is also larger at low luminosities, then larger X-ray features will be produced, as noted above. A larger opening angle is suggested by the greater number of "polarized BEL" Seyfert 2 galaxies compared with BALs (although other origins are possible; see § 6.3).

6.3. *Biconical Structures and the Molecular Torus*

For simplicity we have ignored the presence of accretion disk flaring and of an obscuring molecular torus. If we allow the accretion disk or the torus to cover a large fraction of the sky as seen from the continuum source, then the angles in Figure 1 will be raised toward the axis substantially.

A torus is commonly invoked (Antonucci & Miller 1985; Pier & Krolik 1992) (1) to explain the presence of polarized broad line emission in otherwise narrow-lined (type 2) AGNs (§ 5), (2) to collimate the ionizing radiation that leads to kiloparsec-scale ionization cones of the extended narrow line region (ENLR; Tadhunter & Tsvetanov 1989), and (3) to create the observed 4:1 ratio of obscured (type 2) to unobscured (type 1) AGNs (§ 5). However, direct evidence for a nuclear torus is weak. The maser source in NGC 4258 shows clearly that a thin molecular disk is present in some AGNs down to the 1 pc scale (Greenhill et al. 1995) but does not show that a thick, 2π covering torus is present.

Overall the need for a torus is weaker in this model:

1. We have seen that the Seyfert 2 galaxies with polarized

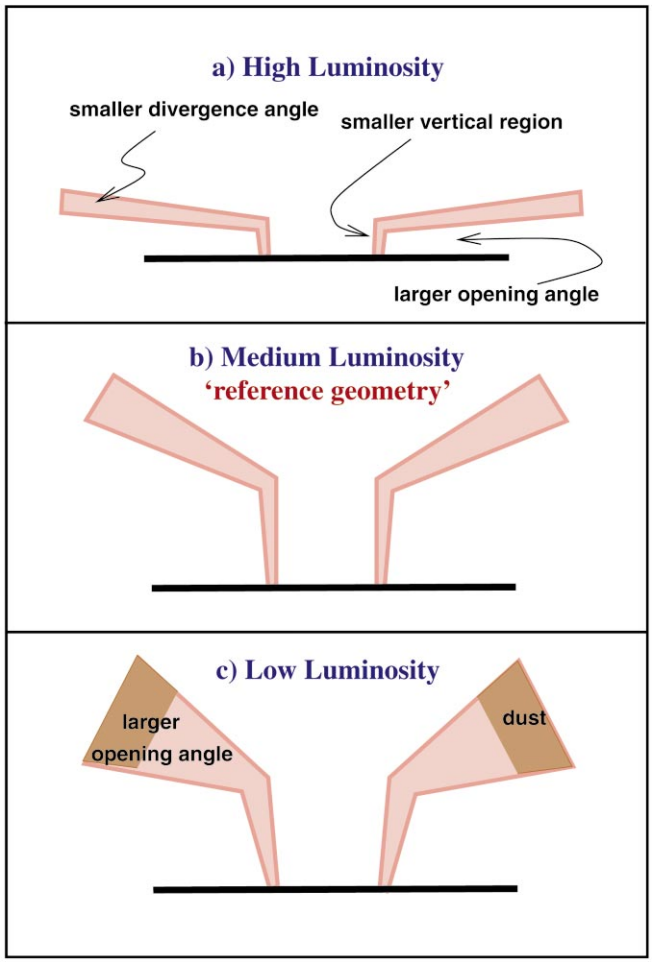

FIG. 7.—Luminosity-dependent changes in the outflow structure that would account for observed luminosity correlations.

BELs could be viewed through a dusty BAL (§ 3.2) and that other, larger scale, asymmetric obscuring structures (e.g., the 70 pc scale warped molecular disk resolved in NGC 1068; Schinnerer et al. 2000) can also produce polarized BEL spectra.

2. The conical shell outflow could itself produce the ENLR bicone structures, which would then be hollow, matter-bounded cones (as suggested by Crenshaw & Kraemer 2000 for NGC 5548), rather than filled, ionization-bounded structures.

3. The other, more common Seyfert 2 galaxies could be made in any of several ways: (a) the large narrow emission line region (NELR) endures $\sim$1000 yr after the central source is extinguished (Lawrence & Elvis 1982), (b) obscuration by large-scale structures in the host galaxy disks (Lawrence & Elvis 1982; Maiolino & Rieke 1995; Simcoe et al. 1998), or (c) in irregular nonnuclear obscuring clouds (Malkan, Gorgian, & Tam 1998) can hide the small BELR but not the much larger NELR in many AGNs.

The structure presented here is not directly inimical to the obscuring torus model, but a torus is less strongly required. The WHIM outflow could in fact be considered as a form of the obscuring torus.

6.4. *Discriminating between Wind Models*

Wind models for quasars have become widely discussed in recent years (see reviews by de Kool 1997; Vestergaard 1999). In particular, the detailed models proposed by Murray et al. (1995) and Murray & Chiang (1995, 1998) and by Cassidy & Raine (1996), as well as the hydrodynamic modeling of Proga, Stone, & Kallman (2000), have many features in common with the empirical picture developed here. This confluence is encouraging. Murray et al. (1995) have a wind emerging from all disk radii and accelerated into a wide cone by radiation pressure, which shows BALs when viewed edge-on. The key geometric difference is that the wind proposed here originates from a narrow range of radii and rises almost vertically before bending outward into a cone. This allows the NALs to be produced by viewing the flow edge-on. The main physical difference is that Murray et al. (1995) and Cassidy & Raine (1996) have a single-phase medium. Murray et al. (1995) have different ionization states being produced from a wide range of footprint radii, producing a radially stratified BELR. The flow proposed here instead forms a two-phase medium that originates in a narrow footprint, and the high- and low-ionization zones are created from shadowing of the continuum by the WHIM in a low-density outer WHIM spanning only a factor of 2 in radius. Ionized absorbers are hard to produce from a radially stratified BELR, unless the density gradient is large (§ 4.1), since we will always be looking through low-ionization material, too, which is X-ray opaque. However, the hydrodynamic models of Proga, Stone, & Drew (1998, 1999) and Proga et al. (2000) show, under some conditions, "streamer"-like high-density structures that resemble the structure proposed here. Detailed calculation may then show that the models are identical.

A related class of models, hydromagnetic wind models, use a magnetic field anchored in the disk to accelerate particles along field lines by centrifugal action (Emmering, Blandford, & Shlosman 1992; Campbell 1999). Bottorf et al. (1997) begin with molecular material that is thrown up from the disk and becomes exposed to the ionizing continuum, thus creating BELs as the clouds are accelerated along the field lines. In these models, as in the Murray et al. (1995) model, the range of radii from which material exits the disk is large.

6.5. *Instabilities and Acceleration*

Several instabilities are known that might create a wind from special radii of an accretion disk. The Lightman-Eardley radiation pressure instability zone in the accretion disk produces a wind originating within a critical instability radius, and the velocities at this radius are comparable to the BELs (Nicastro 2000). The stabilizing effects of a corona may restrict the range of radii in this model. External radiation of the disk can also create a wind from a restricted range of radii at about the correct radius (Begelman, McKee, & Shields 1983; Kurpiewski, Kurasczkiewicz, & Czerny 1997).

Nicastro (2000) also uses in his case an "instability strip" in a disk to explain the range of BEL widths. The radii at which the instability operates changes with $\dot{m}$, the accretion rate relative to the critical Eddington rate. Varying $\dot{m}$ can explain the full range of BEL widths from $\sim$1000 km s^{-1} for narrow-line Seyfert 1 galaxies at high $\dot{m} \sim 1$ to the

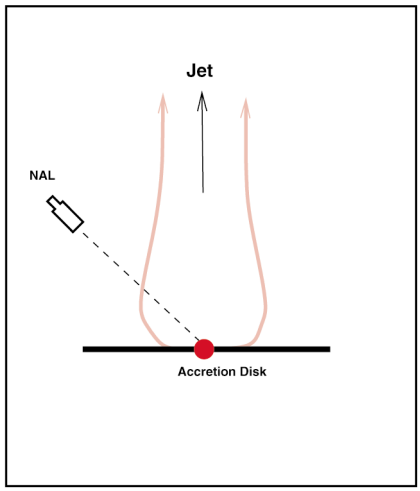

FIG. 8.—Geometry of a recollimated outflow in radio-loud quasars.

broadest lines at $\sim$20,000 km s^{-1}, which occur at the lowest $\dot{m}$ consistent with the disk instability lying outside the minimum stable orbit and where it is able to operate. LINERs may have $\dot{m}$ below this value so that no BELR can form. Changing the radii having the instability will change the opening angle of the flow (§ 4.1). Some luminosity-dependent changes (§ 6.2) may then reflect a more fundamental change in $\dot{m}$. Coupling Nicastro's model with the model presented here seems to explain most of the emission- and absorption-line phenomena in AGNs and quasars.

6.6. *Radio-loud Quasars*

BALs have been found, until recently, only in radio-quiet quasars (Stocke et al. 1992). This suggested quite strongly that the formation of BAL structures was intimately linked with a quasar's radio properties. No such link is implied in the proposed structure. How can we reconcile this disjunction?

There are (at least) three options:

1. Observational bias: Goodrich (1997a) has shown that modest amounts of dust can reduce the observed fraction of BALs by a factor of $\sim$3. So if radio-loud quasars are preferentially dustier than radio-quiet quasars, they would be relatively BAL-free. Such quasars may be reclassified as "radio galaxies" and so dropped from the samples (e.g., 3C 22; Economou et al. 1995). A second effect may be "beaming bias." Even a low-frequency–selected radio sample contains many quasars in which a beamed continuum dominates. These are seen pole-on and, in the proposed structure, would show no absorption. The FIRST survey has now found a substantial fraction of BALs (Becker et al. 1997, 2000; M. Gregg et al. 2000, in preparation) and may be redressing these biases.

2. Jets destroy the BAL outflow: the presence of a relativistic jet will change the environment local to the flow. Cosmic rays or radiation may overionize the flow, reducing the radiation force. Alternatively, the jet radiation or particle pressure may disrupt the outer part of the flow with nonradial forces. Finally, the harder continuum of a radio-loud quasar (Elvis et al. 1994) may be less effective at accelerating the outflow.

3. The most elegant solution is that the outflow recollimates to form the jet. Jets are collimated and accelerated by means that are much debated (e.g., Cellotti & Blandford 2000). Even the scale on which these effects occur is not well determined. It is possible then that, e.g., magnetic fields recollimate the outflow near the point at which it would otherwise be accelerated radially to BAL velocities and instead accelerates the flow toward the poles (§ 6.6) forming the jet. Kuncic (1999) and Vestergaard (1999) make similar proposals. Junor, Biretta, & Livio (1999) see a similar geometry in VLBI observations of M87: a 60° cone out to 100 Schwarzchild radii, where the jet then becomes collimated. The acceleration is then too far from the event horizon to be due to a general relativistic mechanism. If this suggestion is correct, then all radio-loud quasars (apart from those dominated by a beamed continuum) will show NALs (Fig. 8).

7. CONCLUSION

The structure proposed here is clearly ambitious. Yet if we believe that quasars are a solvable problem, some coherent structure must be present. The present proposal, while in strong need of elaboration, draws together previously disparate areas of quasar research into a single simple scheme: the high- and low-ionization parts of the BELR, the BAL and NAL regions, and the five Compton-thick scattering regions can all be combined into the single funnel-shaped outflow. On large scales this outflow could produce the biconical NELRs, and, with small geometric changes, several luminosity-dependent effects can be understood. All of these features come about simply by requiring a geometry and kinematics constructed only to explain the two types of absorption lines. This unification gives the model a certain appeal.

This work has been made possible by the many fascinating and informative discussions I have had with my colleagues and friends at CfA and elsewhere, in particular with Ski Antonucci, Jill Bechtold, Nancy Brickhouse, Massimo Cappi, Bożena Czerny, Giuseppina (Pepi) Fabbiano, Fabrizio Fiore, Margarita Karovska, Andy Lawrence, Smita Mathur, Jonathan McDowell, Norm Murray, Fabrizio Nicastro, Brad Peterson, Richard Pogge, Aneta Siemiginowska, and Meg Urry. The three-dimensional renderings were kindly produced by Antoine Visonneau of the Center for Design Informatics at the Harvard School of Design using the 3D StudioMax software package. This work was supported in part by NASA contract NAS8-39073 (*Chandra* X-ray Center).

REFERENCES

Almaini, O., Boyle, B. J., Griffiths, R. E., Shanks, T., Stewart, G. C., & Georgantopoulos, I. 1995, MNRAS, 277, L31
Antonucci, R., & Miller, J. S. 1985, ApJ, 297, 621
Arav, N., Barlow, T. A., Laor, A., Sargent, W. L. W., & Blandford, R. D. 1998, MNRAS, 297, 990
Baldwin, J. A. 1977, ApJ, 214, 679
Becker, R. H., Gregg, M. D., Hook, I. M., McMahon, R. G., White, R. I., & Helfand, D. J. 1997, ApJ, 479, L93
Becker, R. H., White, R. L., Gregg, M. D., Brotherton, M., Laurent-Muchleisen, S., & Arav, N. 2000, ApJ, 538, 72

Begelman, M. C., McKee, C. F., & Shields, G. A. 1983, ApJ, 271, 70
Beloborodov, A. M., & Poutanen, J. 1999, ApJ, 517, L77
Berriman, G., Schmidt, G. D., West, S. C., & Stockman, H. S. 1990, ApJS, 74, 869
Bottorf, M. C., Korista, K. T., Shlosman, I., & Blandford, R. D. 1997, ApJ, 479, 200
Bromley, B. C., Miller, W. A., & Pariev, V. I. 1998, Nature, 391, 54
Campbell, C. G. 1999, MNRAS, 310, 1175
Capetti, A., Axon, D. J., Macchetto, F. D., Sparks, W. B., & Boksenberg, A. 1996, ApJ, 466, 166
Capetti, A., Macchetto, F. D., & Lattanzi, M. G. 1997, ApJ, 476, L67
Cassidy, I., & Raine, D. J. 1993, MNRAS, 260, 385
———. 1996, A&A, 310, 44
Cellotti, A., & Blandford, R. D. 2000, in Black Holes in Binaries and Galactic Nuclei, ed. L. Kaper, E. P. J. van den Heuvel, & P. A. Woodt (Berlin: Springer), in press
Chiang, J., Reynolds, C. S., Blaes, O. M., Nowak, M. A., Murray, N., Madejski, G., Marshall, H. L., & Magdziarz, P. 2000, ApJ, 528, 292
Cohen, M. H., Ogle, P. M., Tran, H. D., Vermuelen, R. C., Miller, J. S., Goodrich, R. W., & Martel, A. R. 1995, ApJ, 448, L77
Collin-Souffrin, S., Dyson, J. E., McDowell, J. C., & Perry, J. J. 1988, MNRAS, 232, 539
Comastri, A., Setti, G., Zamorani, G., & Hasinger, G. 1995, A&A, 296, 1
Costantini, E., et al. 2000, ApJ, 544, 283
Crenshaw, D. M., & Kraemer, S. B. 1999, ApJ, 521, 572
———. 2000, ApJ, 532, L101
Crenshaw, D. M., Kraemer, S. B., Boggess, A., Marran, S. P., Mushotzky, R. F., & Wu, C.-C. 1999, ApJ, 516, 750
de Kool, M. 1997, in ASP Conf. Ser. 128, Mass Ejection from AGN, ed. N. Arav, I. Shlosman, & R. J. Weymann (San Francisco: ASP), 233
Done, C., Madejski, G. M., & Życki, P. T. 2000, ApJ, 536, 213
Economou, F., Lawrence, A., Ward, M. J., & Blanco, P. R. 1995, MNRAS, 272, L5
Edelson, R. A., Malkan, M. A., & Rieke, G. F. 1987, ApJ, 321, 233
Elvis, M., et al. 1994, ApJS, 95, 1
Emmering, R. T., Blandford, R. D., & Shlosman, I. 1992, ApJ, 385, 460
Espey, B. R., & Andreadis, S. J. 1999, in ASP Conf. Ser. 162, Quasars and Cosmology (San Francisco: ASP), 351
Fabian, A. C., et al. 1994, PASJ, 46, L59
———. 1995, MNRAS, 277, L11
Feldmeier, A., Norman, C., Pauldrach, A., Owocki, S., Puls, J., & Kaper, L. 1997, in ASP Conf. Ser. 128, Mass Ejection from AGN, ed. N. Arav, I. Shlosman, & R. J. Weymann (San Francisco: ASP), 258
Ferland, G. J., Korista, K. T., & Peterson, B. M. 1990, ApJ, 363, L21
Ferland, G. J., Peterson, B. M., Horne, K., Welsh, W. F., & Nahar, S. N. 1992, ApJ, 387, 95
Gallagher, S. C., Brandt, W. N., Sambruna, R. M., Mathur, S., & Yamasaki, N. 1999, ApJ, 519, 549
Georgantopoulos, I., Papadakis, I., Warwick, R. S., Smith, D. A., Stewart, G. C., & Griffiths, R. G. 1999, MNRAS, 307, 815
George, I. M., & Fabian, A. C. 1991, MNRAS, 249, 352
George, I. M., Turner, T. J., & Netzer, H. 1995, ApJ, 438, L67
Goad, R. W., & Koratkar, A. P. 1998, ApJ, 495, 718
Goad, R. W., Koratkar, A. P., Axon, A. J., Korista, K. T., & O'Brien, P. T. 1999, ApJ, 512, L95
Goodrich, R. W. 1997a, in ASP Conf. Ser. 128, Mass Ejection from AGN, ed. N. Arav, I. Shlosman, & R. J. Weymann (San Francisco: ASP), 94
———. 1997b, ApJ, 474, 606
Goodrich, R. W., & Miller, J. S. 1994, ApJ, 434, 82
———. 1995, ApJ, 448, L73
Greenhill, L. J., Jiang, D. R., Moran, J. M., Reid, M. J., Lo, K. Y., & Claussen, M. J. 1995, ApJ, 440, 619
Halpern, J. P., & Moran, E. 1998, ApJ, 494, 194
Hamman, F. 1998, ApJ, 500, 798
Hamann, F., Korista, K. T., & Morris, S. L. 1993, ApJ, 415, 541
Hamann, F., Shields, J. C., Ferland, G. J., & Korista, K. 1995a, ApJ, 454, 688
Hamann, F., Zuo, L., & Tytler, D. 1995b, ApJ, 444, L69
Ho, L. C. 1998, in Observational Evidence for Black Holes in the Universe, ed. S. K. Chakrabati (Dordrecht: Kluwer), 157
Huchra, J. P., & Burg, R. 1992, ApJ, 393, 90
Impey, C. D., Malkan, M. A., Webb, W., & Petry, C. E. 1995, ApJ, 440, 80
Iwasawa, K., & Taniguchi, Y. 1993, ApJ, 413, L15
Junor, W., Biretta, J. A., & Livio, M. 1999, Nature, 401, 891
Kaastra, J. S., Mewe, R., Liedahl, D. A., Komassa, S., & Brinkman, A. C. 2000, A&A, 354, L83
Kaastra, J. S., Roos, N., & Mewe, R. 1995, A&A, 300, 25
Kaspi, S., Brandt, W. N., Netzer, H., Sambruna, R., Chartas, G., Garmire, G. P., & Nousek, J. A. 2000, ApJ, 535, L17
Kay, L. E. 1994, ApJ, 430, 196
Komossa, S. 1999, in ASP Conf. Ser. 175, Structure and Kinematics of Quasar Broad Line Regions, ed. C. M. Gaskell, W. N. Brandt, M. Dietrich, D. Dultzin-Hacyan, & M. Eracleous (San Francisco: ASP), 365
Koratkar, A., Antonucci, R. R. J., Goodrich, R. W., Bushouse, H., & Kinney, A. L. 1995, ApJ, 450, 501
Korista, K. T., et al. 1995, ApJS, 97, 285
Krolik, J. H. 1999, Active Galactic Nuclei (Princeton: Princeton Univ. Press)
Krolik, J. H., & Kriss, G. A. 1995, ApJ, 447, 512
Krolik, J. H., McKee, C., & Tarter, B. 1981, ApJ, 249, 422
Kuncic, Z. 1999, PASP, 111, 954
Kurpiewski, A., Kurasczkiewicz, J., & Czerny, B. 1997, MNRAS, 285, 725
Lawrence, A., & Elvis, M. 1982, ApJ, 256, 410
Lee, J. C., Fabian, A. C., Reynolds, C. S., Brandt, W. N., & Iwasawa, K. 1999, MNRAS, 310, 973
Lee, L. W., & Turnshek, D. A. 1995, ApJ, 453, L61
Lightman, A. P., & White, T. R. 1988, ApJ, 335, 57
Lubinski, P., Zdziarski, A. A., & Madejski, G. M. 2000, Adv. Space Res. (COSPAR), in press
Madejski, G. M., Życki, P., Done, C., Valinia, A., Blanco, P., Rothschild, R., & Turek, B. 2000, ApJ, 535, L87
Maiolino, R., & Rieke, G. H. 1995, ApJ, 454, 95
Malkan, M. A., Gorjian, V., & Tam, R. 1998, ApJS, 117, 25
Maoz, D., Edelson, R., & Nandra, K. 2000, AJ, 119, 119
Marshall, H. L., et al. 1997, ApJ, 479, 222
Mathur, S., Elvis, M., & Singh, K. P. 1996, ApJ, 455, L9
Mathur, S., Elvis, M., & Wilkes, B. J. 1995, ApJ, 452, 230
———. 1999, ApJ, 519, 605
Mathur, S., et al. 2000, ApJ 533, 79L
Mathur, S., Wilkes, B. J., & Elvis, M. 1998, ApJ, 503, L23
Matt, G., Fabian, A. C., & Ross, R. 1991, MNRAS, 262, 179
Matthews, W. G. 1974, ApJ, 189, 23
———. 1986, ApJ, 305, 187
McHardy, I., et al. 1995, MNRAS, 273, 549
Miller, J. S., & Goodrich, R. W. 1990, ApJ, 355, 456
Miller, J. S., Goodrich, R. W., & Mathews, W. 1991, ApJ, 378, 47
Murray, N., & Chiang, J. 1995, ApJ, 454, L105
———. 1998, ApJ, 494, 125
Murray, N., Chiang, J., Grossman, S. A., & Voit, G. M. 1995, ApJ, 451, 498
Nandra, K., George, I. M., Mushotzky, R. F., Turner, T. J., & Yaqoob, T. 1997a, ApJ, 477, 602
———. 1997b, ApJ, 488, L91
Nicastro, F. 1995, Laurea thesis, Univ. Roma "La Sapienza"
———. 2000, ApJ, 530, L65
Nicastro, F., et al. 2000, ApJ, 536, 718
Nicastro, F., Fiore, F., Perola, G. C., & Elvis, M. 1999, ApJ, 512, 184
Ogle, P. M. 1997, in ASP Conf. Ser. 128, Mass Ejection from AGN, ed. N. Arav, I. Shlosman, & R. J. Weymann (San Francisco: ASP), 78
———. 1998, Ph.D. thesis, Caltech
Osmer, P. S., & Shields, J. C. 1999, in ASP Conf. Ser. 162, Quasars and Cosmology (San Francisco: ASP), 235
Osterbrock, D. E. 1989, Astrophysics of Gaseous Nebulae and Active Galactic Nuclei (Mill Valley: Univ. Science Books)
Peterson, B. M. 1993, PASP, 105, 247
———. 1997, An Introduction to Active Galactic Nuclei (Cambridge: Cambridge Univ. Press)
Peterson, B. M., & Wandel, A. 1999, ApJ, 521, L95
Pier, E. A., & Krolik, J. H. 1992, ApJ, 399, L23
Piro, L., Yamauchi, M., & Matsuoka, M. 1990, ApJ, 360, L35
Pounds, K. A., Nandra, K., Stewart, G. C., George, I. M., & Fabian, A. 1990, Nature, 344, 132
Proga, D., Stone, J. M., & Drew, J. E. 1998, MNRAS, 296, L6
———. 1999, MNRAS, 310, 476
Proga, D., Stone, J. M., & Kallman, T. R. 2000, ApJ, 543, 686
Reynolds, C. S. 1997, MNRAS, 286, 513
Rudge, C. M., & Raine, D. J. 1998, MNRAS, 297, L1
Rush, B., Malkan, M. A., & Spinoglio, L. 1993, ApJS, 89, 1
Schild, R. E. 1996, ApJ, 464, 125
Schinnerer, E., Eckart, A., Tacconi, L. J., Genzel, R., & Downes, D. 2000, ApJ, 533, 850
Schmidt, G. D., & Hines, D. C. 1999, ApJ, 512, 125
Shields, J. C. 1994, in ASP Conf. Ser. 69, Reverberation Mapping of the Broad-Line Region in Active Galactic Nuclei, ed. P. M. Goodhalekar, K. Horne, & B. M. Petterson (San Francisco: ASP), 293
Shields, J. C., Ferland, G. J., & Peterson, B. M. 1995, ApJ, 441, 507
Shull, M. J., & Sachs, E. R. 1993, ApJ, 416, 536
Simcoe, J. A., McLeod, K. K., Schachter, J., & Elvis, M. 1998, ApJ, 489, 615
Stocke, J. J., Morris, S. L., Weymann, R. J., & Foltz, C. B. 1992, ApJ, 396, 487
Tadhunter, C., & Tsvetanov, Z. 1989, Nature, 341, 422
Tanaka, Y., et al. 1995, Nature, 375, 659
Telfer, R. C., Kriss, G. A., Zheng, W., Davidsen, A. F., & Green, R. F. 1998, ApJ, 509, 132
Turner, T. J., Nandra, K., George, I. M., Fabian, A. C., & Pounds, K. A. 1993, ApJ, 419, 127
Turnshek, D. A. 1988, in QSO Absorption Lines: Probing the Universe, ed. J. C. Blades, D. A. Turnshek, & C. A. Norman (Cambridge: Cambridge Univ. Press), 17
Turnshek, D. A., Kopko, M., Monier, E., Noll, D., Espey, B. R., & Weymann, R. J. 1996, ApJ, 463, 110
Vestergaard, M. 1999, Ph.D. thesis, Niels Bohr Institute for Astronomy, Physics and Geophysics, Copenhagen Univ.
Vignali, C., Comastri, A., Nicastro, F., Matt, G., Fiore, F., & Palumbo, G. G. C. 2000, A&A, in press (astro-ph/0008090)
Weymann, R. J. 1997, in ASP Conf. Ser. 128, Mass Ejection from AGN, ed. N. Arav, I. Shlosman, & R. J. Weymann (San Francisco: ASP), 3

Weymann, R. J., Morris, S. L., Foltz, C. B., & Hewett, P. C. 1991, ApJ, 373, 23
Wilkes, B. J. 1984, MNRAS, 207, 73
Williams, R. J. R. 2000, MNRAS, 316, 803
Witt, H. J., Czerny, B., & Życki, P. T. 1997, MNRAS, 286, 848
Young, S., Corbett, E. A., Giannuzzo, M. E., Hough, J. H., Robinson, A., Bailey, J. A., & Axon, D. J. 1999, MNRAS, 303, 227
Życki, P. T., & Czerny, B. 1994, MNRAS, 266, 653